https://chemclassjournal.com/
ChemClass Journal Vol. 9 Issue 4 (2025); 92 - 114
e-ISSN:3092-8214 p-ISSN:3092-8206
doi.org/10.33003/chemclas_2025_0904/08

In vitro Antimicrobial Efficacy of Chitosan Nanoparticles-Encapsulated *Balanites aegyptiaca* Leaf Extract

Chol Abraham Lual*[,1, 2], Benjamin Asen Anhwange[1,2], C. A. Adah[1,2],

[1]*Department of Chemistry, Benue State University, Makurdi, Nigeria*
[2]*Centre for Food Technology and Research, Benue State University, Makurdi, Nigeria*

***Corresponding author:** Email: +2349119243142; lual19@bsum.edu.ng
Co-author[1]: +2348057050242; banhwange@bsum.edu.ng
Co-author[2]: +2347069037034; caadah@bsum.edu.ng.

Abstract

The study focuses on the antimicrobial effectiveness and the physicochemical properties of chitosan nanoparticles-encapsulated *Balanites aegyptiaca* leaf extract. Gas Chromatography - Mass Spectrometry (GC-MS) was employed for the phytochemical analysis of *B. aegyptiaca* leaf extract, whereas Fourier Transform InfraRed (FT-IR), Dynamic Light Scattering (DLS), X-ray Diffraction (XRD), Scanning Electron Microscopy (SEM), and Thermal Gravimetric Analysis (TGA) were used for characterization of chitosan nanoparticles and the nanoencapsulated extracts. The antimicrobial effectiveness against Gram-positive, Gram-negative bacteria, and fungi was assessed using the agar-well diffusion method. The GC-MS analysis of the extract identified 18 compounds, including alkaloids, terpenoids, and phenolics. The FT-IR spectra of the encapsulated extract revealed the functional groups present, indicating successful encapsulation. DLS analysis revealed that the particle sizes were at the nanoscale (323.3 nm and 296.3 nm) with low polydispersity (0.301 and 0.317) for the nanoparticles and nanoencapsulated extracts, respectively. In contrast, XRD analysis showed a decrease in crystallinity in the encapsulated extract. SEM images presented spherical, monodispersed nanoparticles, and TGA indicated that the extract's thermal stability improved with nanoencapsulation. Antimicrobial tests revealed that the crude extract exhibited strong activity against *Pectobacterium carotovorum*, with inhibition zones of 26.23 mm, surpassing that of chloramphenicol at 18.20 mm. The nanoencapsulation enhanced antimicrobial effectiveness, showing greater inhibition zones (22.20 mm) and lower MICs (1.563–3.125 mg/mL) across the test pathogens, including gram-positive (B. subtilis, L. plantarum), gram-negative (S. syringae), and fungal (S. cerevisiae) species. These results emphasise the potential of nanoencapsulated *Balanites aegyptiaca* as natural antimicrobial agents for post-harvest loss control and pharmaceutical applications.

Keywords: Chitosan, Nanoencapsulation, *Balanites aegyptiaca*, Phytochemicals, Antimicrobial Agent, post-harvest loss.

1.0 Introduction

The tomato (*Solanum lycopersicum L.*) is highly susceptible to spoilage due to its high moisture content and delicate texture. This perishability leads to significant post-harvest losses. especially in regions with limited cold chain infrastructure, affecting food security and economic losses for

© CSN Zaria Chapter

farmers [1]. There are bacterial and fungal pathogens responsible for the tomato spoilage, including *Pseudomonas syringae*, *Pectobacterium carotovorum, Bacillus subtilis*, and *Saccharomyces cerevisiae,* among others [2, 3]. Therefore, finding an effective, natural, sustainable preservation method for tomatoes is a pressing scientific and practical challenge. One promising approach involves exploring medicinal plants that have been used for centuries to treat numerous illnesses [4]. These plants contain secondary metabolites that can inhibit harmful microorganisms, and they may serve as an alternative to overcome stubborn microorganisms [5, 6].

Balanites aegyptiaca, commonly known as the desert date, is a recognized medicinal plant. This tree is indigenous to the arid and semi-arid regions of Africa and the Middle East. It has maintained traditional medicine systems for ages, with recorded applications against infectious diseases, metabolic disorders, and inflammatory conditions [7]. Ethnopharmacological surveys reveal extensive utilization across geographical regions: Sudanese utilize aqueous leaf extracts for treating skin infections and fever [8, 9, 10], while Nigerian traditional healers incorporate the leaves in formulations targeting sexually transmitted infections, and Ethiopian communities utilize leaf decoctions for gastrointestinal disorders [11].

The therapeutic efficacy of *B. aegyptiaca* is attributed to its rich phytochemical profile, comprising saponins, flavonoids, alkaloids, and phenolic compounds that collectively provide antimicrobial, antifungal, anti-inflammatory, and antioxidant properties [7]. Previous studies have reported the extract's inhibitory activity against relevant pathogens, including *Klebsiella pneumoniae* and *Staphylococcus aureus*, with minimum inhibitory concentrations of 12 mg/mL and 25 mg/mL, respectively [12]. However, the clinical translation of plant-based antimicrobial bioactive compounds has limitations, mainly poor physicochemical stability and uncontrolled release, which limit their therapeutic efficacy [13].

Nanotechnology-based drug delivery systems have emerged as transformative solutions to overcome these limitations. Among various nanocarriers, chitosan nanoparticles have drawn attention due to their biocompatibility, biodegradability, and antimicrobial activity [14]. The cationic nature of chitosan, derived from chitin deacetylation, enables electrostatic interactions with negatively charged bacterial cell membranes, enhancing antimicrobial efficacy while providing a sustainable alternative to synthetic preservatives [15, 16]. Moreover, the high surface area-to-volume ratio in nanoparticles enhanced bioactive compound encapsulation, improved stability, and controlled release [17].

Nanoencapsulation technology represents a paradigm shift in natural product delivery, offering protection against environmental degradation while enabling targeted and sustained release of bioactive compounds [18]. This

approach involves the encapsulation of liquid or solid samples within protective matrices, forming natural nanocapsules that are eco-friendly [19, 20]. The ionic gelation method has been successfully employed to encapsulate plant extracts within the chitosan structure [21].

Despite the therapeutic capability of *B. aegyptiaca* and the advantages offered by chitosan nanoencapsulation, the poor stability and controlled release of their bioactive components remain a limitation. The present study addresses this knowledge gap by evaluating the antimicrobial effectiveness and physicochemical characteristics of chitosan nanoparticles-encapsulated *B. aegyptiaca* leaf extract against the tomato spoilage microorganisms.

2.0 Materials and Methods

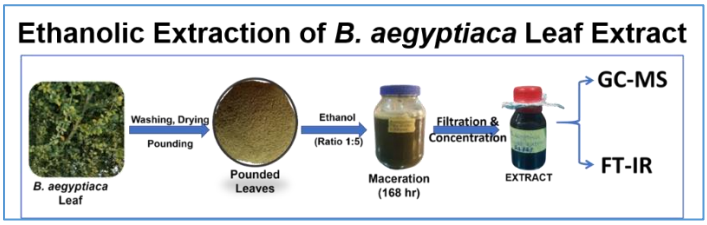
2.1. Sample Collection and Preparation

2.1.1. Sample Collection

The *Balanites aegyptiaca* leaves were collected from Bor, Jonglei State, South Sudan. The leaves were washed thoroughly with distilled water and shade-dried to a constant weight for two weeks at room temperature, ensuring preservation of thermolabile compounds. The dried leaves were pulverized using a mortar and pestle and sieved over a 0.2 mm mesh to give a fine particle size to maximize solvent penetration during extraction. This was stored inside a zip-lock bag for further use [22]. African freshwater mussel shells were purchased from the Wurkum market of Makurdi town, Benue State, Nigeria. The shells were thoroughly washed with distilled water, sun-dried, pulverized, sieved over a 0.2 mm mesh, and kept in a zip-locked bag.

2.1.2. Ethanolic Extraction

Ground dry leaf sample (500 g) was homogenized and macerated in a stoppered container with 2.5 L of 80 % v/v at a 1:5 (w/v) plant-to-solvent ratio, and then left to stand at ambient temperature for 168 hours. The extract was filtered through a funnel with filter paper, followed by concentration using a water bath at 80°C for 4 hours to obtain the crude extract, and stored in an amber bottle until further use [23].



Scheme 1: Extraction of B. aegyptiaca Leaf Bioactive Compounds using the Maceration Method

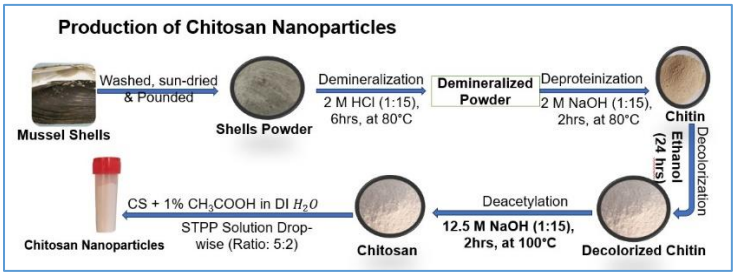
2.1.3. Extraction of Chitin from Mussel Shells

Following the John et al. (2020) [24], chitin extraction protocol. The demineralization process was achieved by treating 1.0 gram of the African freshwater mussel shells pulverized sample with 2M HCl in a 1:15 weight-to-volume ratio for 6 hours at 80°C with continuous stirring on a hot plate. The residue was deproteinized using 2M NaOH (1:15 w/v) at 80°C with continuous stirring on a hot plate for 6 hours. The discoloration of the

sample was achieved by immersing it in 98% pure ethanol for 24 hours. The resulting chitin was dried at 25°C for 72 hours. The deacetylation process was performed by heating the chitin with 12.5M NaOH (1:15 w/v) at 100°C with continuous stirring on a hot plate for 4 hours to produce chitosan. After each stage (demineralization, deproteinization, discoloration, and deacetylation), the product was filtered, washed, and rinsed with distilled water until reaching neutral pH 7. The final chitosan product was dried at 25°C for 72 hours and stored in a zip-lock bag.

2.1.4. Preparation of Chitosan-Nanoparticles

A 0.5 g (500 mg) of chitosan was dissolved in 100 mL of (1% v/v) acetic acid solution in deionized water. A solution of 5mg/mL Sodium Tripolyphosphate (STPP) was prepared by dissolving 0.5 g of STPP in 100 mL of deionized water, as outlined by [25]. To 100 mL of chitosan solution, 40 mL of the prepared Sodium tripolyphosphate (STPP) solution was added dropwise at 1 mL/min with continuous stirring. The mixture was then centrifuged at 3,000 rpm for 90 minutes. The pellet nanoparticles were washed with distilled water, air-dried for 72 hours, and stored in a zip-lock bag [26].

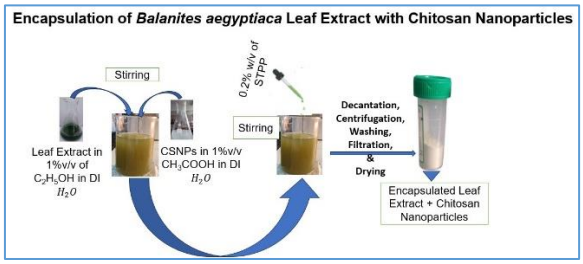


Scheme 2: Production of Chitosan Nanoparticles from Mussel Shells using Ion Gelation Method

2.1.5. Encapsulation of *B. aegyptiaca* Leaf Extract with Chitosan Nanoparticles

Chitosan nanoparticles were bound to the leaf extract by modifying the ionic gelation procedure. A 0.5g of chitosan nanoparticles was dissolved in 100 mL of 0.5% v/v glacial acetic acid solution, stirred thoroughly until dissolved, then filtered to remove the impurities and undissolved particles. In 100 mL of deionized water, a 0.5g STTP solution (0.2% w/v) was dissolved. In 100 mL of deionized water, 0.5g of *Balanites aegyptiaca* leaf extract (0.1% w/v) was dissolved. A 20 mL of *Balanites aegyptiaca* leaf extract was added to the 100 mL of chitosan-glacial acetic solution and stirred thoroughly for 15 minutes. Then, 40 mL of STPP solution was added dropwise into the leaf extract-chitosan-glacial acetic acid solution while maintaining continuous agitation. The ratio of the chitosan-STPP-Leaf extract solution was kept constant at 5:2:1 during the experimentation. After the STPP solution had been fully added, the mixture was further stirred for 30 minutes to complete the reaction to form stable nanoparticles. To isolate the *B.*

aegyptiaca/chitosan-linked nanoparticles from the supernatant, they were centrifuged at 3,000 rpm for 90 minutes. The nanoparticle pellets were collected and washed with deionized water to remove any remaining free components. The purified nanoparticles were air-dried for 72 hours and stored in a zip-lock bag [26].



Scheme 3: Encapsulation of *B. aegyptiaca* Leaf Extract with Chitosan Nanoparticles using Ion Gelation Method

2.2. Characterization

2.2.1. Determination of Phytochemical Composition of *B. aegyptiaca* Leaf Extract

According to the Standard analytical protocols outlined by Mwangi et al. (2024) [27]. The leaf extract sample was analysed using the gas chromatograph equipped with a capillary column (30 m, 0.25 mm, i.e., film thickness 0.25 µm) and coupled to a mass selective detector. The oven temperature was held at 50 °C, then raised by 7 °C/min to 300 °C, and the injector temperature was 290 °C. Helium was used as the carrier gas with a flow rate of 1 mL/min, and the split ratio was 60:1. Mass spectra was obtained at 60 eV ionization energy. The leaf extract sample of 10 µL was diluted with 990 µL of n-hexane, and 1 µL was injected for the analysis. The identification of the components in the sample was done by comparing their retention index and mass fragmentation patterns with those available in the National Institute of Standards and Technology (NIST) library [28].

2.2.2. Determination of Functional Groups Composition of *B. aegyptiaca* Leaf Extract

The functional groups of *B. aegyptiaca* Leaf Extract, Chitosan Nanoparticles (CHN), and Chitosan Nanoparticles encapsulated with *B. aegyptiaca* leaf extract (BCH) were characterized using a Fourier Transform Infrared (FT-IR) Spectrophotometer (Thermo-Scientific Nicolet iS10, Waltham, USA) as outlined by Mwangi et al [29]. Approximately 1 mg of each sample was mixed with inert potassium bromide in a 1:50 ratio and ground to achieve uniformity. The mixture was then compressed using the FT-IR hand-press equipment to prepare a translucent pellet, and the pellet was mounted on the instrument's sample holder for analysis of its functional groups. Various absorption bands within the 4000- 600 cm^{-1} range were recorded.

2.2.3. Determination of Size Distribution

Dynamic Light Scattering (DLS) analysis was used to study the size distribution of chitosan nanoparticles and chitosan-*Balanite aegyptiaca*'s leaf extract nanoparticles based on the Brownian motion of particles in suspension. After setting the DLS (PN3702 Zetasizer, Malvern, UK) instrument at a scattering angle of 90° at 25 °C, 10 mL of the encapsulated nanoparticle solution

was poured into a clean cuvette and inserted into the DLS instrument. The measurement duration was 60 seconds, with several repetitions averaged for enhanced precision [30].

2.2.4. Determination of Crystallinity

The crystallinity of prepared chitosan, chitosan nanoparticles, and chitosan-*Balanite aegyptiaca*'s leaf extract nanoparticles was determined by X-ray diffractometry (XRD) by the method described by Kaewprachu et al. (2023) [31] using BRUKER-D2 PHRASER XRD Diffractometer (Bruker GmbH, Germany). The data was evaluated within the 2θ range of 5–80°.

2.2.5. Determination of Surface Morphology

The surface morphology of Chitosan, chitosan nanoparticles, and *B.* aegyptiaca Leaf Extract loaded with Chitosan nanoparticles were observed with SEM (MERLIN-ZEISS GmbH, Germany) at magnification 20,000x and 50,000x [32].

2.2.6. Determination of Thermal Stability

The thermal stability of chitosan nanoparticles and chitosan nanoparticles encapsulating *B. aegyptiaca* were determined following the method described by [33] using TGA (PerkinElmer, Shelton, CT, USA) for the thermal stability, composition, and degradation profile of nanoparticles by measuring weight changes as a function of temperature. A sample of 20 mg of dried nanoparticle powder was placed in a clean, pre-weighed sample pan. The sample was heated from room temperature to 800°C at a rate of 15°C per minute in an inert nitrogen atmosphere at a flow rate of 40 mL/min to prevent oxidation. The weight changes were recorded continuously to produce a thermogram, which was analyzed to identify decomposition steps and determine the thermal stability of the samples.

2.3. Antimicrobial Assay

2.3.1. Microbial Strains

Six microbial strains were selected to represent the microbial targets: Gram-negative bacteria (*Pseudomonas syringae* ATCC 19310, *Pectobacterium carotovorum* subsp. *carotovorum* ATCC 39048), Gram-positive bacteria (*Bacillus subtilis* ATCC 6051, *Lactobacillus plantarum* ATCC 14917), and fungi (*Penicillium chrysogenum* ATCC 10106, *Saccharomyces cerevisiae* ATCC 9763).

2.3.2. Determination of Zone of Inhibition

The agar-well diffusion technique was employed for the antimicrobial assay, as adopted from Mohammed and Kuhiyep [34]. From inoculum stocks of each test isolate, a 1 mL aliquot was withdrawn using a sterile micropipette with fixed tips and dispensed into sterile, properly labelled disposable petri dishes. The plates were pour-plated with molten but cool Mueller-Hinton Agar and Sabouraud Dextrose Agar. Once solidified, the agar was aseptically punched with a sterile 8 mm cork-borer to create centralized wells, and the agar plugs were carefully placed, avoiding tears

to the well edges. The test agents (100 µL) were loaded in the wells. The positive control consisted of 0.01 mg/L of Chloramphenicol (bacteria) and 0.02 mg/L of Voriconazole (fungi), while the negative control was the diluent. Inhibition zones were measured using digital callipers with ±0.01 mm precision from the disk edge to the margin of complete growth inhibition, with each treatment done in triplicate.

2.3.3. Determination of Minimum Inhibitory Concentration /Dilution for MIC/MBC/MFC

The broth-dilution technique described by Obunukwu et al. (2018) [35] was used. Two-fold dilution for the extract and the nanoparticles with sterile distilled water, yielding different concentrations (1.563 – 12.50 mg/L). Distilled water and broth medium served as negative controls, while the positive controls were chloramphenicol (Bacteria) and ketoconazole (Fungi) in appropriate Mueller-Hinton Broth (MHB). Inoculum (100 µL) of standardized microbial suspension was added to each 5 mL serially-placed test tube containing medium, except the controls, before incorporation of 100 µL antimicrobial agent. Incubation was at 35°C, 24 hours for bacteria and 32°C, 72 hours for fungi. The turbidity of sets (indicating microbial proliferation) was compared, and the least turbid tube with relative clarity was selected as the MIC. The clear tubes were subsequently pour-plated into isolation medium (nutrient agar or potato dextrose agar) to establish a biocidal concentration as needed. All experimental setups were performed in triplicate (n = 3).

2.4. Statistical Analysis and Data Validation

All experiments followed a randomized design with three independent biological replicates for antimicrobial assays. Data were reported as the mean ± SD of three replicate measurements using SPSS 28.0.

3.0 Results and Discussion

3.1. Results

3.1.1. Phytochemical Composition of *B. aegyptiaca* Leaf Extract

The GC-MS analysis of the ethanolic leaf extract of *B. aegyptiaca* revealed 18 compounds comprising fatty acids, terpenoids, sterols, and other organic constituents. Among the identified compounds, fatty acid was the most abundant group (**Table 1**).

Table 1: The phytochemical profiling of *Balanite aegyptiaca* leaf using GC-MS

Library/ID	Classes
2,4-dimethyl-Benzo[h]quinoline	Alkaloids
5-methyl-2-phenyl-1H-Indole	Alkaloids
3,5,7-Triamino-1-azaadamantane	Alkaloids
2-Ethylacridine	Alkaloids
tetrahydro-6-undecyl-2H-Pyran-2-one	Flavonoids
2-(n-Propyl)oxybenzylidene acetophenone	Flavonoids
2-(2-Methylpropyl)oxybenzylidene acetophenone	Flavonoids
5,7-Dimethyloctahydrocoumarin	Flavonoids
4-hydroxy-3,5,6-trimethyl-4-(3-oxo-1-butenyl)-2-Cyclohexen-1-one	Flavonoids
alpha.-Tocopherol-.beta.-D-mannoside	Saponins
1,4,6-Trimethyl-1,2,3,3a,4,7,8,8a-octahydro-4,7-ethanoazulene	Terpenoids
Neophytadiene	Terpenoids
2,2,4-Trimethyl-3-pentanol	Terpenoids
2-Hydroxy-4-methoxy-7-methyl-7,8,9,10,11,12,13,14-octahydro-6-oxabenzocyclododecen-5-one	Terpenoids
gamma.-Tocopherol	Terpenoids
2,6,10,14,18-Pentamethyl-2,6,10,14,18-eicosapentaene	Terpenoids
Stigmasterol	Steroids
Phytol	Steroids

3.1.2. Functional Groups Composition of *B. aegyptiaca* Leaf Extract

The FTIR spectrum of *B. aegyptiaca* Leaf Extract, Chitosan Nanoparticles, and Chitosan Nanoparticles Encapsulated *B. aegyptiaca* Ethanolic Leaf Extract revealed characteristic absorption bands corresponding to key functional groups of bioactive compounds **(Figure 2)**.

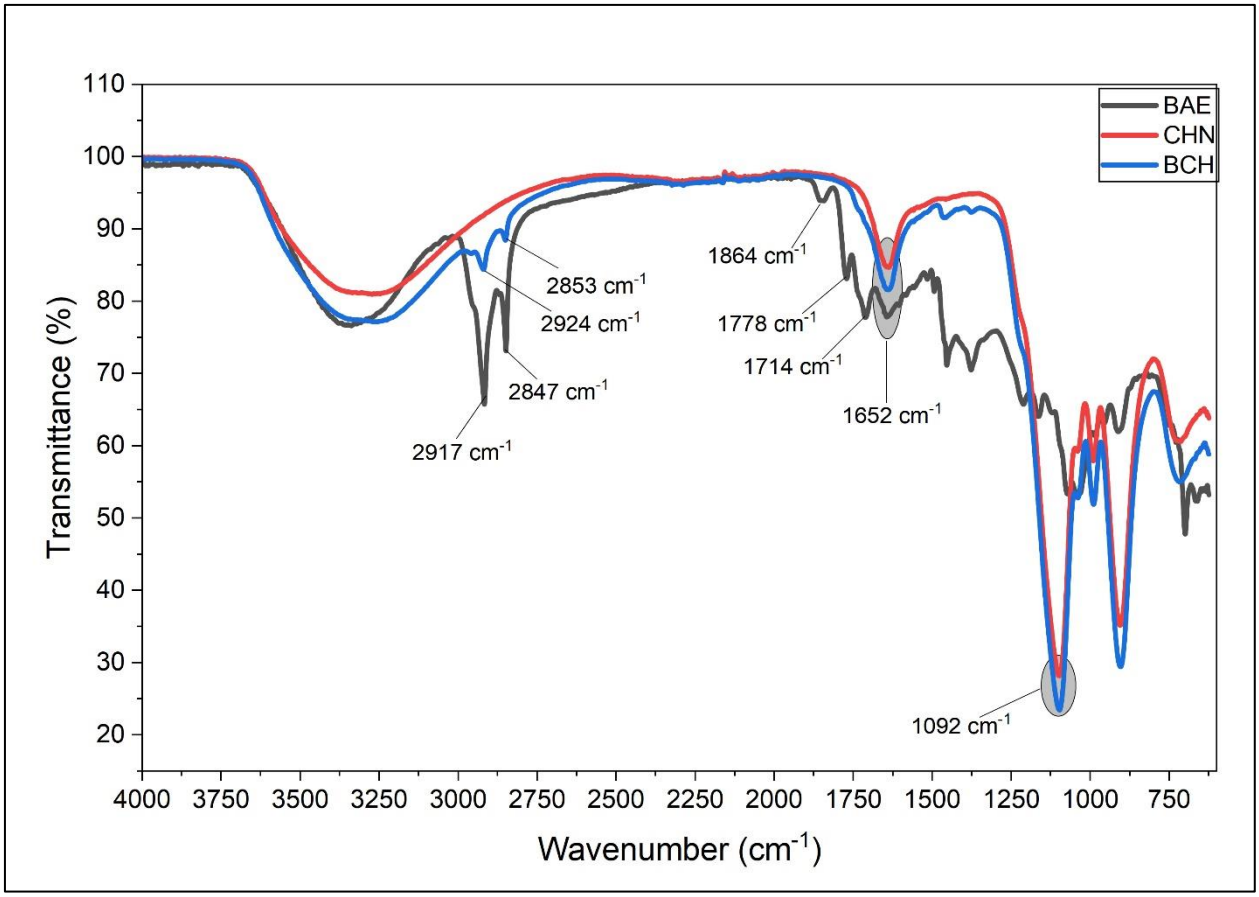


Figure 1: FTIR Spectral Analysis of *B. aegyptiaca* Leaf Extract, Chitosan Nanoparticles, and Chitosan Nanoparticles Encapsulated *B. aegyptiaca* Ethanolic Leaf Extract

3.1.3. Size Distribution

Figure 2 shows Size Distribution of Chitosan Nanoparticles and Chitosan Nanoparticles Encapsulated *B. aegyptiaca* Ethanolic Leaf Extract analyses through DLS.

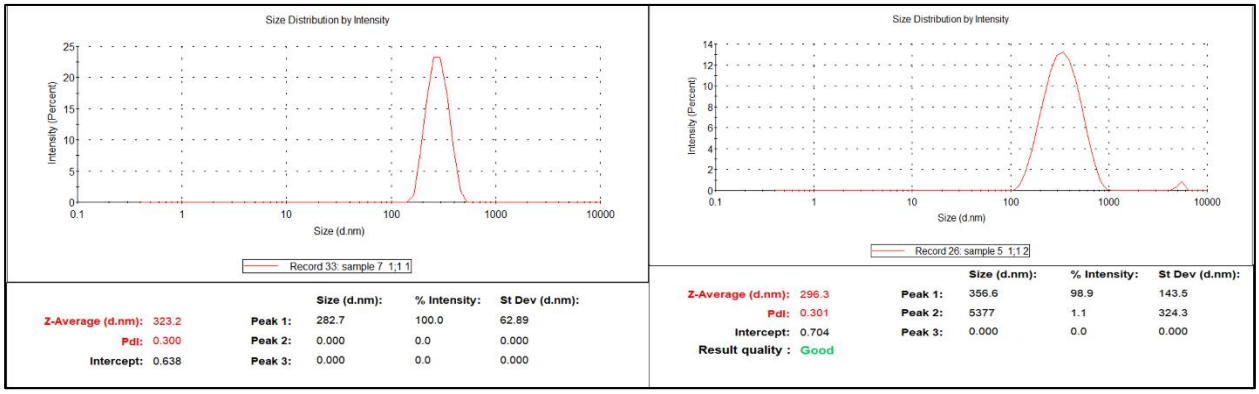


Figure 2: DLS for Size Distribution of Chitosan Nanoparticles (Sample 7) and Chitosan Nanoparticles Encapsulated *B. aegyptiaca* Ethanolic Leaf Extract (Sample 5)

3.1.4. Structural Crystallinity

The crystalline properties of the Chitosan Nanoparticles (CHN) and the Chitosan Nanoparticles loaded with *B. aegyptiaca* leaf extract (BCH) were examined using X-ray diffraction (XRD), and the resulting patterns are presented in **Figure 3**.

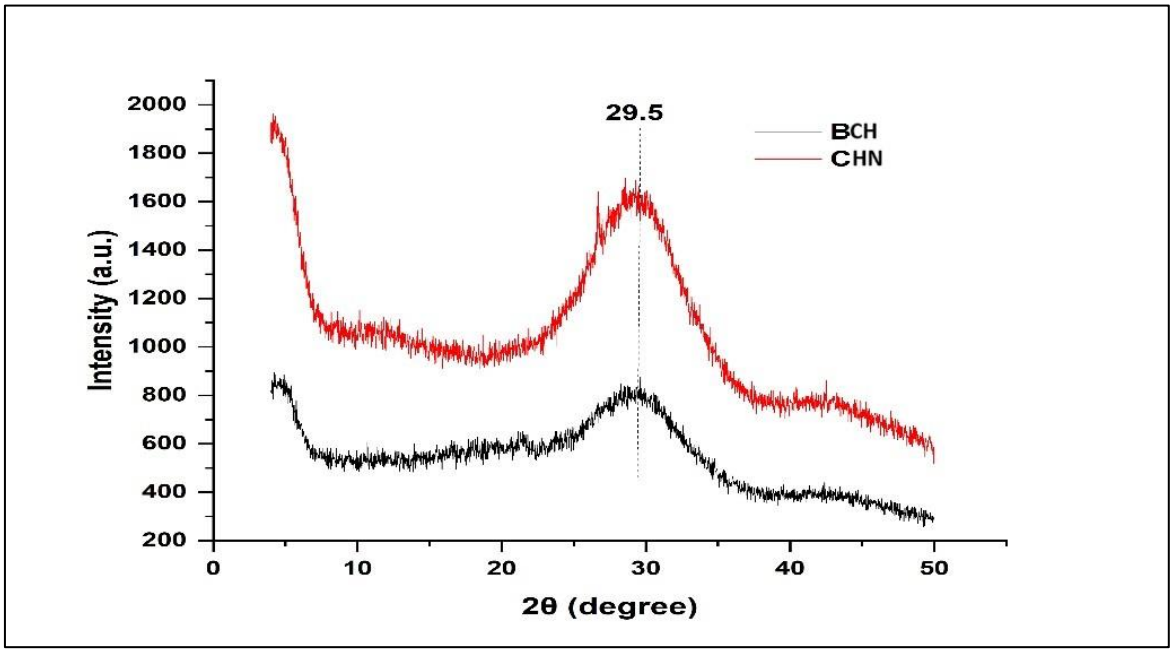


Figure 3: XRD patterns of chitosan nanoparticles (CHN) and *B. aegyptiaca* Leaf Extract-loaded chitosan nanoparticles.

3.1.5. Surface Morphology

Figure 4 shows the morphology of Chitosan Nanoparticles (CHN) and Chitosan Nanoparticles encapsulated with *B. aegyptiaca* Leaf Extract (BCH) at 20 KX and 50 KX.

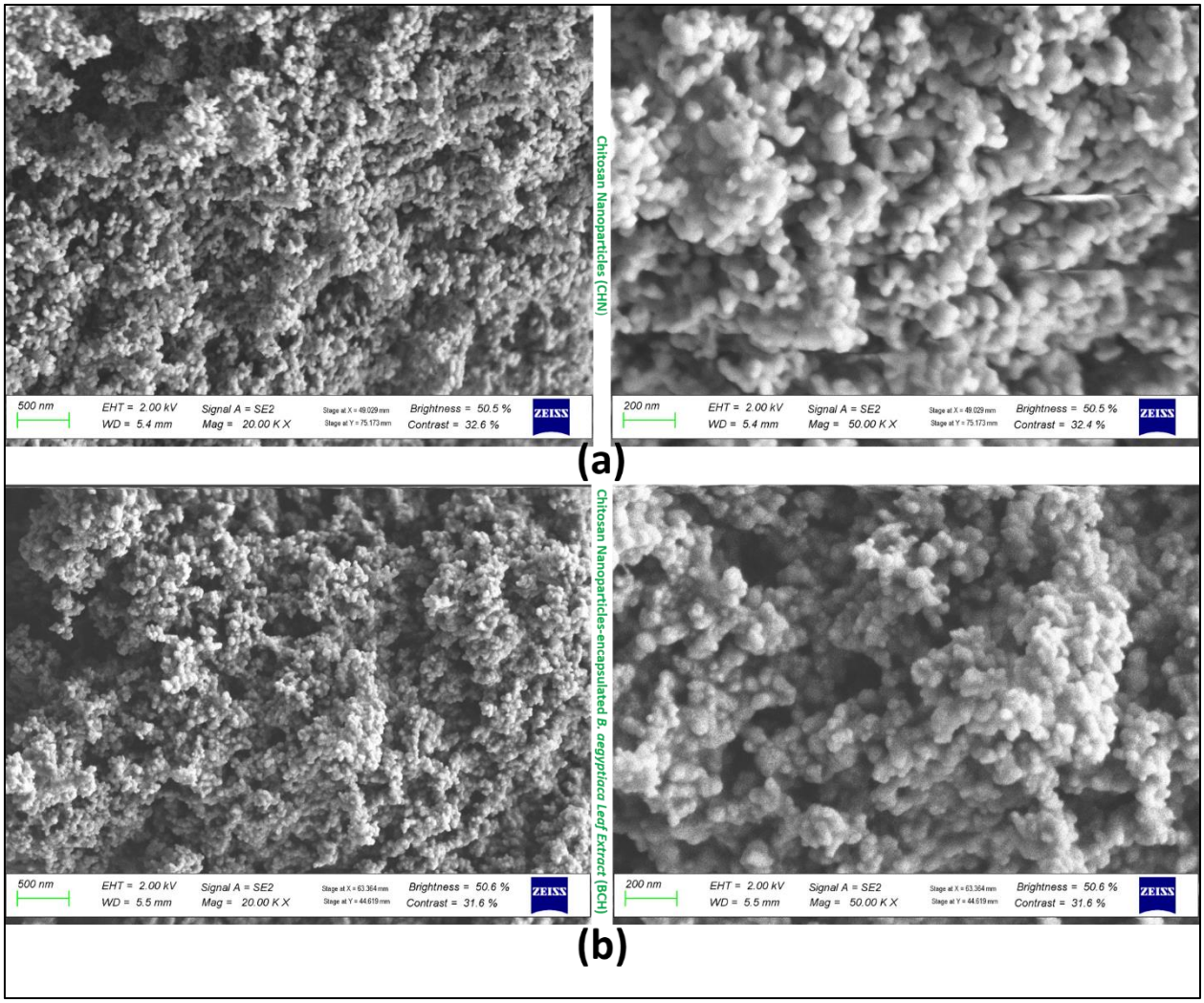


Figure 4: Morphology of (a) Chitosan Nanoparticles (CHN) and (b) Chitosan Nanoparticles encapsulated with *B. aegyptiaca* Leaf Extract (BCH) through SEM analysis.

3.1.6. Thermal Stability

Figure 5 shows the Thermograms of chitosan nanoparticles (CHN) and chitosan nanoparticles loaded with *B. aegyptiaca* leaf extract (BCH).

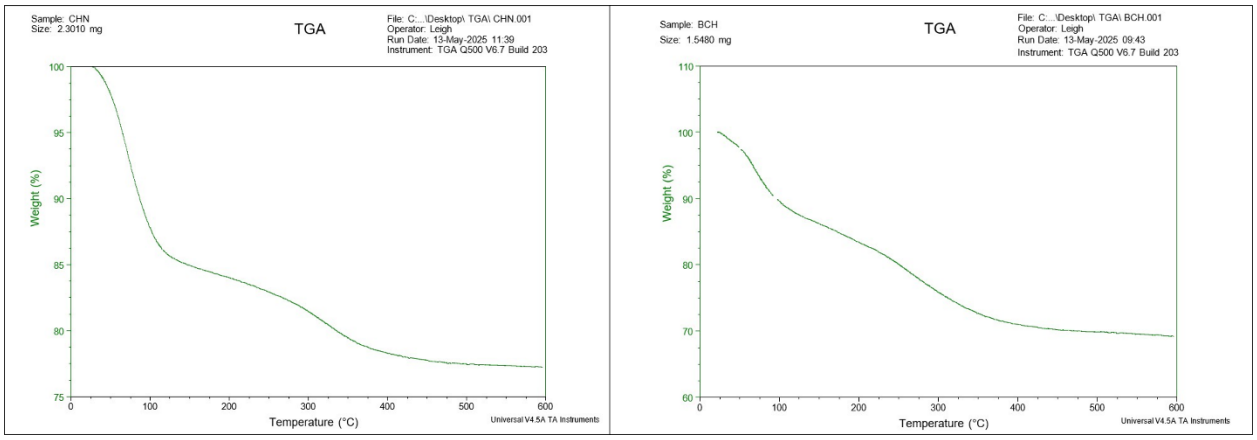


Figure 5: The TGA curves showing the degradation of chitosan nanoparticles (CHN) and chitosan nanoparticles-encapsulated *B. aegyptiaca* leaf extract (BCH)

3.1.3. Antimicrobial Assay

The zone of inhibition reveals the susceptibility of test organisms to antimicrobial agents, indicating the efficacy against microbial growth. In this study, *Balanites aegyptiaca* leaf extract (BAE), Chitosan Nanoparticles (CHN), and Chitosan Nanoparticles Encapsulated *Balanites aegyptiaca* leaf extract (BCH) were tested against six pathogens: *Bacillus subtilis*, *Lactobacillus plantarum*, *Pseudomonas syringae*, *Pectobacterium carotovorum*, *Penicillium notatum*, and *Saccharomyces cerevisiae*. The results presented in **Table 2** demonstrate that BAE exhibited varying degrees of antimicrobial activity, ranging from low to high inhibition zones.

Table 2: **Zone of Inhibition (Antimicrobial Effectiveness) of *B. aegyptiaca* Leaf Extract (BAE), Chitosan Nanoparticles (CHN), and Chitosan Nanoparticles Encapsulated with *B. aegyptiaca* leaf extract (BCH) against Test Pathogens**

Type	Test Microorganism	Zone of Inhibition (mm)			Chloramphenicol (0.01mg/L)	Ketoconazole (0.02mg/L)
		BAE (50 mg/L)	CHN (50 mg/L)	BCH (50 mg/L)		
Gram-positive Bacteria	*Bacillus subtilis*	12.10	11.14	11.13	18.21	
	Lactobacillus plantarum	18.20	13.14	15.13	19.17	
Gram-negative Bacteria	*Pseudomonas syringae*	10.13	11.9	14.10	21.26	
	Pectobacterium carotovorum	26.23	17.18	22.20	18.20	
Fungi	*Penicillium notatum*	10.12	12.14	8.10		23.20
	Saccharomyces cerevisiae	15.17	13.20	12.11		20.19

Values indicate the susceptibility of test microorganisms

Table 3: Minimum Inhibitory and Biocidal Concentrations (mg) of the Antimicrobial *B. aegyptiaca* leaf extract (BAE), Chitosan Nanoparticles (CHN), and Chitosan Nanoparticles Encapsulated with *B. aegyptiaca* leaf extract (BCH) against Test Pathogens.

Type	Test Organism	BAE			CHN			BCH		
		MIC	MBC	MFC	MIC	MBC	MFC	MIC	MBC	MFC
Gram-positive Bacteria	*B. subtilis*	3.13	12.5		6.25	12.5		1.56	12.5	
	L. plantarum	1.56	6.25		1.56	3.13		3.13	6.25	
Gram-negative Bacteria	*P. syringae*	1.56	6.25		1.56	6.25		3.13	12.5	
	P. carotovorum	3.13	6.25		1.56	3.13		6.25	12.5	
Fungi	*P. notatum*	6.25		-	6.25		-	12.5		-
	S. cerevisiae	3.13		12.5	1.56		6.25	3.13		-

(-) indicates no detection of biocidal effectiveness across assayed concentrations (**unit in mg/L**)

3.2. Discussion

3.2.1. Phytochemical Composition of *B. aegyptiaca* Leaf Extract

The GC-MS analysis indicated a total of 18 phytochemicals, including alkaloids, terpenoids, saponins, steroids, phenolic compounds, and fatty acids from *B. aegyptiaca* leaf crude extract, similar to the findings by Murthy *et al*. [7] who reported secondary metabolites, including alkaloids, saponins, polyphenols, steroids, and glycosides isolated from seeds, leaves, stem bark, and roots of *B. aegyptiaca*. The analysis revealed that alkaloids such as 1H-indole, 5-methyl-2-phenyl-, 2-ethylacridine, benzo[h]quinoline, 2,4-dimethyl-, and 3,5,7-triamino-1-azaadamantane [28]**.** The flavonoids present were 5,7-dimethyloctahydrocoumarin, 2-cyclohexen-1-one derivatives, and 2-(n-propyl)oxybenzylidene acetophenone [36]**.** Phenolic acids like 2-butenoic acid, 4-hydroxy-, methyl ester were also identified [37]. Other classes present in low quantities were saponins [38] and steroids like stigmasterol [39]**.**

3.2.2. Functional Groups Composition of *B. aegyptiaca* Leaf Extract

The FT-IR spectra showed strong peaks that verify the functional groups present in BAE, CHN, and the encapsulated BCH. All three samples exhibited a broad absorption band in the region of 3300-3400 cm^{-1}, indicating the

presence of O-H stretching vibrations, likely from hydroxyl groups in organic compounds [41, 42]. The absorption bands between 2924 and 2853 cm^{-1} (with additional peaks at 2917 cm^{-1} and 2847 cm^{-1}) are linked to the aliphatic C–H stretching of CH_3 [42]. The peaks at 1714 cm^{-1}, 1778 cm^{-1}, and 1864 cm^{-1} agree with the C=O stretching vibrations of ester or carbonyl group [44, 45]. A peak at 1652 cm^{-1} is coupled with amide I (C=O) stretching in biopolymer, which originates from Chitosan Nanoparticles [45]. The peak at 1092 cm^{-1} corresponds to C–O–C and C–O stretching associated with the glycosidic linkages present in the glucose unit of Chitosan Nanoparticles [46]. The shifts and changes in intensity observed in the BCH spectrum, compared to the individual components, suggest successful chemical interactions, such as hydrogen bonding and the presence of BAE bioactive compounds within the nanoencapsulated sample matrix [18].

3.2.3. Size Distribution

The CHNs showed a peak at 274.4 nm with an intensity of 100%. This indicates a consistent particle size distribution with minimal aggregation, supported by a PDI of 0.317 [47], [48]. The average sizes of 323.3 nm for CHNs and 296.3 nm for BCHs are within the nanoscale range reported for chitosan nanoparticles [30]. The low PDI values of 0.301 and 0.317 confirm fine size distributions, which are key for confirming stable biological applications [49].

3.2.4. Structural Crystallinity

The samples exhibit a broad diffraction peak centred at about $2\theta = 29.5°$, which is characteristic of the semi-crystalline nature of chitosan-based materials [50]. The CHN band shows a sharper and more intense peak, indicating higher crystallinity. Upon encapsulation of the *B. aegyptiaca* leaf extract (BAE), there was a decrease in crystallinity observed with peak intensity drop and broadening of the diffraction signal, as shown in **Figure 3**. Plant extracts have been shown to weaken the ability of the chitosan chains to align into a highly ordered crystalline structure, thereby increasing the proportion of amorphous regions [52, 53].

3.2.5. Surface Morphology

The SEM micrographs demonstrate morphological differences between the chitosan nanoparticles (CHN) and those encapsulated with *Balanites aegyptiaca* leaf extract. The CHNs (**Figure 4a**) appear spherical and monodispersed with smooth surfaces at 50, 000 X magnification, showing a successful ionic gelation process [53]. This uniform spherical shape agrees with the studies done by [54], who reported the observed spherical morphology of the nanoparticles using SEM, indicating their regular distribution. BAE-loaded CHN displayed surface roughness and agglomerations as observed in **Figure 4b.** These results relate to [55] findings, which showed nanoparticles-encapsulated *Ginkgo biloba* extract with an aggregate of spherical and

rough particles with coarse surface. The surface changes after nanoencapsulation suggest successful incorporation of the extracts on the nanocarrier [56].

3.2.6. Thermal Stability

Figure 5 shows the TGA thermograms of chitosan nanoparticles (CHN) and chitosan nanoparticles-encapsulated *B. aegyptiaca* leaf extract (BCH). It can be observed that both samples exhibited mass loss in two stages. The first stage mass loss occurred below 100 °C due to evaporation of moisture, and the loss of some nonencapsulated compounds of the *B. aegyptiaca* extracts by El-Naggar et al. [59], according to the decomposition of encapsulated *M. oleifera* compounds, which usually occurred between 135 and 320 °C. The second stage involved mass loss above 300 °C due to the degradation and breakdown of functional groups, such as the OH group present on the chitosan nanoparticles chains. These results agree with the report of El-Naggar et al. [59], who observed that the decomposition of phenolic compounds and polymers occurs between 350 and 450 °C. All the samples showed almost similar weight loss, but the extract-encapsulated had a mass residue of about 30% above 500 °C, a better thermal stability compared to chitosan nanoparticles with a mass residue of approximately 15% above 500 °C. These findings are related to the observations by George et al. [60], who also revealed that encapsulation of *M. oleifera* bioactive compounds enhances their thermal stability.

3.2.7. Antimicrobial Assay

The Gram-negative pathogen *P. carotovorum* showed high susceptibility to crude *Balanites aegyptiaca* leaf extract (BAE), with inhibition zones measuring 26.23 mm, surpassing the chloramphenicol (positive control), which had a zone of 18.20 mm. Both CHN and BCH also exhibited antibacterial activities against the *P. carotovorum*, with inhibition zones of 22.20 mm and 17.18 mm, respectively. This performance of BAE may be due to the combined action of bioactive compounds like saponins, alkaloids, and polyphenols [59]. On the other hand, *P. syringae* exhibited lower susceptibility to all treatments, with inhibition zones ranging from 10.13 to 14.10 mm, compared to the control (chloramphenicol's 21.26 mm). This species-specific resistance might have originated from differences in the composition of outer membrane lipopolysaccharides, which can hinder antimicrobial penetration.

However, the nanoencapsulated BCH particles showed improved efficacy [60]. There was moderate activity against Gram-positive bacteria, *L. plantarum* with inhibition zones ranging from 12.10-18.20 mm and *B. subtilis* with inhibition zones ranging from 11.14 to 12.10 mm. These results are consistent with earlier studies that indicated a preference for Gram-positive strains, suggesting that the effectiveness of antimicrobial agents is more about specific phytochemical profiles than broad taxonomic categories [61].

The Antifungal testing showed some differences in susceptibility. *P. notatum* was the most susceptible to CHN, measuring 12.14 mm, followed by BAE at 10.12 mm and BCH at 8.10 mm. This supports the known fungicidal activities of chitosan [62]. Also, *S. cerevisiae* showed greater susceptibility across all treatments, with BAE at 15.17 mm, CHN at 13.20 mm, and BCH at 12.11 mm. This aligns with recent research revealing the capability of chitosan nanoparticles for controlling microorganisms [57]. The antifungal differences in the results could be related to species-specific differences in cell wall structure and membrane permeability [7].

Among the three treatments, BCH showed the highest antibacterial efficacy with the lowest MIC values. Against Gram-positive bacteria (*B. subtilis*), CHN showed an excellent range of activity against *L. plantarum* (MIC: 1.56 mg/L, MBC: 6.25 mg/L) but reduced efficacy against *B. subtilis* (MIC: 6.25 mg/L). The crude *B. aegyptiaca* leaf extract (BAE) exhibited moderate activity with MIC values of 1.56 mg/L against *L. plantarum* and 3.13 mg/L against *B. subtilis*, corresponding to MBC values of 6.25 mg/mL for both organisms. These results are related to the previous studies reporting plant extract MIC ranges of 0.625 mg/L to 2.5 mg/L against oral pathogens [63]. The encapsulated treatment (BCH) showed efficacy with species-specific variations: higher efficacy against *B. subtilis* (MIC: 1.56 mg/L) than *L. plantarum* (MIC: 3.13 mg/L). Against Gram-negative pathogens, CHN maintained consistent high efficacy with MIC values of 1.56 mg/L against both *P. carotovorum* and *P. syringae*, achieving low MBC values of 1.56 mg/L, revealing bactericidal activity at the same concentration as growth inhibition. BAE displayed a difference in activity with the highest efficacy against *P. syringae* (MIC: 1.56 mg/L) compared to *P. carotovorum* (MIC: 3.13 mg/L), while both showed the same MBC values of 6.25 mg/L. The encapsulated chitosan nanoparticles-*B. aegyptiaca* Leaf extract (BCH) treatment exhibited reverse selectivity, showing better activity against *P. carotovorum* (MIC: 3.13 mg/L) than *P. syringae* (MIC: 6.25 mg/L), with higher MBC values of 12.5 mg/L for both species.

The enhanced activity of encapsulated nanoparticles treatment could result from improved cellular penetration and sustained release mechanisms [64]. Antifungal screening showed species-specific susceptibility patterns across all treatments. CHN displayed the highest antifungal efficacy with MIC values of 1.56 mg/L against *S. cerevisiae* and 6.25 mg/L against *P. notatum*, achieving fungicidal activity against *S. cerevisiae* at 6.25 mg/L concentration. This excellent performance highlights chitosan's established mechanism of membrane disruption and intracellular interference in fungal cells [65]. Both BAE and BCH showed the same MIC patterns against *S. cerevisiae* (3.13 mg/L) but different in their performances against *P. notatum* (BAE: 6.250 mg/L vs. BCH: 12.5 mg/L). There was no MFC detected for *P. notatum* across all

treatments, indicating fungistatic rather than fungicidal activity against this species. The observed antifungal efficacy supports previous findings with plant extracts, the ethanolic extracts showing fungal inhibition [66].

4.0 Conclusion

This study highlighted the antimicrobial properties of chitosan nanoparticles-encapsulated *Balanites aegyptiaca* leaf extract. *Pectobacterium carotovorum* was shown to be the most susceptible pathogen among the other tested bacteria and fungi. The nanoencapsulation of *Balanites aegyptiaca* Leaf Extract with chitosan nanoparticles enhanced the antimicrobial effectiveness, showing greater inhibition zones of (11.13 to 22.20 mm). The lowest MIC for the nanoencapsulated *Balanites aegyptiaca* leaf extract was found to be between (1.563 – 3.125 mg/L) on specific microorganisms across the test pathogens of gram-positive (*S. subtilis*, *L. plantarum*), gram-negative (*S. syringae*), and fungi (*S. cerevisiae*). Nanoencapsulation was also observed to have improved the thermal stability of the extracts, as observed in TGA analysis. These results suggest potential application of chitosan nanoparticles-encapsulated *Balanites aegyptiaca* leaf extract as natural antimicrobial agents for food preservation and biomedical uses. Future research can focus on *in vivo* tests on the chitosan nanoencapsulated *B. aegyptiaca* leaf extract for food preservation.

Funding

This research was facilitated under the German Academic Exchange Service (DAAD) In-Region/In-country Scholarship Program.

Conflict of Interest

The authors declare no conflicts of interest associated with this work.

Data Availability

The authors hereby declare that all the data used in this work have been supplied in the manuscript.

Acknowledgements

The first author is grateful to the German Academic Exchange Services (DAAD) and the Centre for Food Technology and Research (CEFTER) for logistics and technical support.

References

[1] M. M. Urugo *et al.*, "Addressing post-harvest losses through agro-processing for sustainable development in Ethiopia," *Journal of Agriculture and Food Research*, p. 101316, 2024.

[2] O. Lastochkina *et al.*, "Bacillus spp.: efficient biotic strategy to control postharvest diseases of fruits and vegetables," *Plants*, vol. 8, no. 4, p. 97, 2019, Accessed: Nov. 02, 2025. [Online]. Available: https://www.mdpi.com/2223-7747/8/4/97

[3] S. Sharmin, "Post Harvest Diseases Of Some Selected Salad Vegetables, Their Causes And Management," PhD Thesis, DEPARTMENT OF PLANT PATHOLOGY, 2020. Accessed: Nov. 02, 2025. [Online]. Available: https://archive.saulibrary.edu.bd/handle/123456789/3274

[4] M. N. AlZain, F. M. Albarakaty, and R. M. A. El-Desoukey, "An Ethnobotanical, Phytochemical Analysis, Antimicrobial and Biological Studies of Pulicaria crispa as a Graze Promising Shrub," *Life*, vol. 13, no. 11, p. 2197, 2023, doi: 10.3390/life13112197.

[5] K. Keita, C. Darkoh, and F. Okafor, "Secondary plant metabolites as potent drug candidates against antimicrobial-resistant pathogens," *SN Applied Sciences*, vol. 4, no. 8, 2022, doi: 10.1007/s42452-022-05084-y.

[6] M. Arip *et al.*, "Review on plant-based management in combating antimicrobial resistance-mechanistic perspective," *Frontiers in Pharmacology*, vol. 13, p. 879495, 2022.

[7] H. N. Murthy, G. G. Yadav, Y. H. Dewir, and A. Ibrahim, "Phytochemicals and biological activity of desert date (Balanites aegyptiaca (L.) Delile)," *Plants*, vol. 10, no. 1, p. 32, 2020.

[8] S. Borehalli Mayegowda *et al.*, "Eco-friendly synthesized nanoparticles as antimicrobial agents: an updated review," *Frontiers in Cellular and Infection Microbiology*, vol. 13, no. August, pp. 1–13, 2023, doi: 10.3389/fcimb.2023.1224778.

[9] I. B. Abubakar *et al.*, "Traditional medicinal plants used for treating emerging and re-emerging viral diseases in northern Nigeria," *European Journal of Integrative Medicine*, vol. 49, p. 102094, 2022.

[10] M. Yu, I. Gouvinhas, J. Rocha, and A. I. R. N. A. Barros, "Phytochemical and antioxidant analysis of medicinal and food plants towards bioactive food and pharmaceutical resources," *Scientific Reports*, vol. 11, no. 1, pp. 1–14, 2021, doi: 10.1038/s41598-021-89437-4.

[11] M. E. Osawaru and M. C. Ogwu, "Plants used in the management and treatment of female reproductive health issues: case study from southern Nigeria," in *Herbal Medicine Phytochemistry: Applications and Trends*, Springer, 2024, pp. 1013–1049.

[12] D. Kulawe, N. Ahidjo, and J. S. Hena, "The Ethanolic Extracts of the Root, Stem and Leaves of Balanites aegyptiaca against Selected Microbes," *Asian Journal of Biotechnology and Bioresource Technology*, vol. 5, no. 4, pp. 1–7, 2019, doi: 10.9734/ajb2t/2019/v5i430067.

[13] S. Alahmer, M. El-Noss, and A. Farid, "Preparation of chitosan nanoparticles loaded with Balanites aegyptiaca extract for treatment of streptozotocin-induced diabetes in rats," *International Journal of Biological Macromolecules*, vol. 262, no. P2, p. 130061, 2024, doi: 10.1016/j.ijbiomac.2024.130061.

[14] A. El-Araby, W. Janati, R. Ullah, S. Ercisli, and F. Errachidi, "Chitosan, chitosan derivatives, and chitosan-based nanocomposites: eco-friendly materials for advanced applications (a review)," *Frontiers in Chemistry*, vol. 11, no. January, pp. 1–21, 2023, doi: 10.3389/fchem.2023.1327426.

[15] E. Akdaşçi, H. Duman, F. Eker, M. Bechelany, and S. Karav, "Chitosan and Its Nanoparticles: A Multifaceted Approach to Antibacterial Applications," *Nanomaterials*, vol. 15, no. 2, pp. 1–41, 2025, doi: 10.3390/nano15020126.

[16] K. Wu *et al.*, "Recent Advances in the Preparation, Antibacterial Mechanisms, and Applications of Chitosan," *Journal of Functional Biomaterials*, vol. 15, no. 11, 2024, doi: 10.3390/jfb15110318.

[17] P. Poznanski, A. Hameed, and W. Orczyk, "Chitosan and Chitosan Nanoparticles: Parameters Enhancing Antifungal Activity," *Molecules*, vol. 28, no. 7, 2023, doi: 10.3390/molecules28072996.

[18] M. Soltanzadeh, S. H. Peighambardoust, B. Ghanbarzadeh, M. Mohammadi, and J. M. Lorenzo, "Chitosan nanoparticles as a promising nanomaterial for encapsulation of pomegranate (Punica granatum l.) peel extract as a natural source of antioxidants," *Nanomaterials*, vol. 11, no. 6, 2021, doi: 10.3390/nano11061439.

[19] J. L. Guía-García *et al.*, "Micro and nanoencapsulation of bioactive compounds for agri-food applications: A review," *Industrial Crops and Products*, vol. 186, p. 115198, 2022.

[20] R. D. C. Díaz-Torres, A. J. Alonso-Castro, M. L. Carrillo-Inungaray, and C. Carranza-Alvarez, "Bioactive compounds obtained from plants, their pharmacological applications and encapsulation," in *Phytomedicine*, Elsevier, 2021, pp. 181–205.

[21] M. Pateiro *et al.*, "Nanoencapsulation of promising bioactive compounds to improve their absorption, stability, functionality and the appearance of the final food products," *Molecules*, vol. 26, no. 6, 2021, doi: 10.3390/molecules26061547.

[22] G. C. Ezemokwe, J. C. Aguiyi, and F. P. Chollom, "The Antibacterial Activity of Aqueous and Ethanolic Leaf Extracts of Balanites aegyptiaca (l.) Del Plant on Some Selected Clinical Human Pathogens," *Journal of Advances in Microbiology*, vol. 20, no. 10, pp. 51–66, 2020, doi: 10.9734/jamb/2020/v20i1030290.

[23] A. P. Cacique, É. S. Barbosa, G. P. de Pinho, and F. O. Silvério, "Maceration extraction conditions for determining the phenolic compounds and the antioxidant activity of catharanthus roseus (L.) g. don," *Ciencia e Agrotecnologia*, vol. 44, pp. 1–12, 2020, doi: 10.1590/1413-7054202044017420.

[24] K. John Kasongo, D. J. Tubadi, L. D. Bampole, T. A. Kaniki, N. J. M. Kanda, and M. E. Lukumu, "Extraction and characterization of chitin and chitosan from Termitomyces titanicus," *SN Appl. Sci.*, vol. 2, no. 3, p. 406, Mar. 2020, doi: 10.1007/s42452-020-2186-5.

[25] A. Rahman *et al.*, "Green Synthesized Chitosan Nanoparticles for Controlling Multidrug-Resistant mecA-and blaZ-Positive Staphylococcus aureus and aadA1-Positive Escherichia coli," *International Journal of Molecular Sciences*, vol. 25, no. 9, p. 4746, 2024.

[26] N. Zein *et al.*, "In vivo investigation of the anti-liver fibrosis impact of Balanites aegyptiaca/chitosan nanoparticles," *Biomedicine & Pharmacotherapy*, vol. 172, p. 116193, 2024.

[27] J. W. Mwangi, D. Kiragu, and B. Chaka, "Phytochemical screening, FTIR and GCMS analysis of Cucurbita pepo seeds cultivated in Kiambu county, Kenya," *Heliyon*, vol. 10, no. 9, 2024, Accessed: Nov. 04, 2025. [Online]. Available: https://www.cell.com/heliyon/fulltext/S2405-8440(24)06268-6

[28] B. Ali, "Expanding the Use of Gas Chromatography–Mass Spectrometry for Untargeted Bioanalysis of Volatile Metabolites," Master's Thesis, Arizona State University, 2024. Accessed: Nov. 04, 2025. [Online]. Available: https://search.proquest.com/openview/8692ec2efccaa3de9830426b24e3caa6/1?pq-origsite=gscholar&cbl=18750&diss=y&casa_token=Q3SB-Ty4y-4AAAAA:7F-I-nJ3Z9V2XAcCmdAQUqePoe6gmBXHpjiu6B1qlTba19gmuFY0Is58Gc9BrhLtttdsu8R88ansgw

[29] J. W. Mwangi, D. Kiragu, and B. Chaka, "Phytochemical screening, FTIR and GCMS analysis of Cucurbita pepo seeds cultivated in Kiambu county, Kenya," *Heliyon*, vol. 10, no. 9, 2024.

[30] J. Rodriguez-Loya, M. Lerma, and J. L. Gardea-Torresdey, "Dynamic Light

Scattering and Its Application to Control Nanoparticle Aggregation in Colloidal Systems: A Review.," *Micromachines*, vol. 15, no. 1, Dec. 2023, doi: 10.3390/mi15010024.

[31] P. Kaewprachu and C. Jaisan, "Physicochemical Properties of Chitosan from Green Mussel Shells (Perna viridis): A Comparative Study," *Polymers*, vol. 15, no. 13, pp. 1–14, 2023, doi: 10.3390/polym15132816.

[32] L. Zhao *et al.*, "Effects of different drying methods on the characterization, dissolution rate and antioxidant activity of ursolic acid-loaded chitosan nanoparticles," *Foods*, vol. 10, no. 10, 2021, doi: 10.3390/foods10102470.

[33] A. A. Yaqoob, S. H. Sekeri, M. B. H. Othman, M. N. M. Ibrahim, and Z. H. Feizi, "Thermal degradation and kinetics stability studies of oil palm (Elaeis Guineensis) biomass-derived lignin nanoparticle and its application as an emulsifying agent," *Arabian Journal of Chemistry*, vol. 14, no. 6, p. 103182, 2021, doi: 10.1016/j.arabjc.2021.103182.

[34] S. S. D. Mohammed and C. Y. Kuhiyep, "Bacteria and fungi co-biodeterioration of selected fresh tomatoes sold within Ungwan Rimi, Kaduna," *Science World Journal*, vol. 15, no. 1, pp. 48–55, 2020, Accessed: Nov. 04, 2025. [Online]. Available: https://www.ajol.info/index.php/swj/article/view/203080

[35] G. M. Obunukwu, K. S. Dike, and G. E. Nwakwasi, "Isolation and identification of microbial deteriogens of fresh tomatoes stored at ambient temperature," *Microbiology Research Journal International*, vol. 26, no. 1, pp. 1–8, 2018, Accessed: Nov. 04, 2025. [Online]. Available: https://www.researchgate.net/profile/Gift-Obunukwu/publication/330031571_Isolation_and_Identification_of_Microbial_Deteriogens_of_Fresh_Tomatoes_Stored_at_Ambient_Temperature/links/6775517ae74ca64e1f4027f8/Isolation-and-Identification-of-Microbial-Deteriogens-of-Fresh-Tomatoes-Stored-at-Ambient-Temperature.pdf

[36] Y. L. Powder-George and F. K. Mohammed, "GC-MS analysis of the bioactive phytoconstituents of various organic crude extracts from the seed kernels of Manilkara bidentata (balata) collected in Trinidad, WI," *Natural Product Research*, vol. 32, no. 3, pp. 358–361, 2018.

[37] P. O. Tedela, "Phytochemical Profiling and GC-MS Analysis of Extracts of Two Tropical Moss Species," *Scholars Academic Journal of Biosciences*, vol. 11, no. 05, pp. 181–190, 2023, doi: 10.36347/sajb.2023.v11i05.003.

[38] P. P. Rao *et al.*, "Evaluation of the merit of ethanolic extract of Annona reticulata as an anti-cancer agent in human colon cancer cell lines (HCT-116)," *F1000Research*, vol. 12, pp. 1–20, 2024, doi: 10.12688/f1000research.141542.2.

[39] K. Kasman, N. I. Ishak, P. Hastutiek, E. Suprihati, and ..., "Identification of Active Compounds of Ethanol Extract of Citrus amblycarpa leaves by Analysis of Thin layer Chromatography and Gas Chromatography," *Macedonian Journal*, vol. 8, pp. 1–6, 2020.

[40] M. O. Yusuf, "Bond Characterization in Cementitious Material Binders Using Fourier-Transform Infrared Spectroscopy," *Applied Sciences (Switzerland)*, vol. 13, no. 5, 2023, doi: 10.3390/app13053353.

[41] D. S. Volkov, O. B. Rogova, and M. A. Proskurnin, "Temperature dependences of ir spectra of humic substances of brown coal," *Agronomy*, vol. 11, no. 9, 2021, doi: 10.3390/agronomy11091822.

[42] J. Sharifi-Rad *et al.*, "Chitosan nanoparticles as a promising tool in

nanomedicine with particular emphasis on oncological treatment," *Cancer Cell International*, vol. 21, no. 1, pp. 1–21, 2021, doi: 10.1186/s12935-021-02025-4.

[43] M. S. Alqahtani *et al.*, "Preparation, characterization, and in vitro-in silico biological activities of Jatropha pelargoniifolia extract loaded chitosan nanoparticles," *International journal of pharmaceutics*, vol. 606, p. 120867, 2021.

[44] M. R. Wylie and D. S. Merrell, "The Antimicrobial Potential of the Neem Tree Azadirachta indica," *Frontiers in Pharmacology*, vol. 13, no. May, pp. 1–16, 2022, doi: 10.3389/fphar.2022.891535.

[45] M. Constantin *et al.*, "PVA/Chitosan Thin Films Containing Silver Nanoparticles and Ibuprofen for the Treatment of Periodontal Disease," *Polymers*, vol. 15, no. 1, 2023, doi: 10.3390/polym15010004.

[46] B. Gieroba *et al.*, "Surface Chemical and Morphological Analysis of Chitosan/1,3-β-D-Glucan Polysaccharide Films Cross-linked at 90 °C," *International Journal of Molecular Sciences*, vol. 23, no. 11, pp. 1–23, 2022, doi: 10.3390/ijms23115953.

[47] K. M. Zia, "Characterization Techniques for the Chitosan Nanoparticles and Derivatives," in *Chitosan*, Springer, 2025, pp. 135–176.

[48] J. D. A. Villarta, F. J. C. Paylago, J. C. H. Poldo, J. S. R. Santos, T. A. M. M. Escordial, and C. M. Montealegre, "Green Synthesis, Characterization, and Optimization of Chitosan Nanoparticles Using Blumea balsamifera Extract," *Processes*, vol. 13, no. 3, 2025, doi: 10.3390/pr13030804.

[49] N. König *et al.*, "Stability of Nanopeptides: Structure and Molecular Exchange of Self-assembled Peptide Fibers," *ACS Nano*, vol. 17, no. 13, pp. 12394–12408, 2023, doi: 10.1021/acsnano.3c01811.

[50] E. Alehosseini, H. Shahiri Tabarestani, M. S. Kharazmi, and S. M. Jafari, "Physicochemical, thermal, and morphological properties of chitosan nanoparticles produced by ionic gelation," *Foods*, vol. 11, no. 23, p. 3841, 2022, Accessed: Nov. 04, 2025. [Online]. Available: https://www.mdpi.com/2304-8158/11/23/3841

[51] M. Hasan, A. Utami, C. Siregar, L. Hanum, I. Khaldun, and M. Nazar, "Thermal, structural and mechanical characterization of bio-nanocomposite films from purple sweet potato starch/chitosan nanoparticles integrated with anthocyanin extract," *Results in Engineering*, vol. 25, no. February, p. 104448, 2025, doi: 10.1016/j.rineng.2025.104448.

[52] S. A. Al-Hilifi, R. M. Al-Ali, and A. T. Petkoska, "Ginger Essential Oil as an Active Addition to Composite Chitosan Films: Development and Characterization," *Gels*, vol. 8, no. 6, 2022, doi: 10.3390/gels8060327.

[53] M. Sathiyabama *et al.*, "Green synthesis of chitosan nanoparticles using tea extract and its antimicrobial activity against economically important phytopathogens of rice," *Scientific Reports*, vol. 14, no. 1, pp. 1–10, 2024, doi: 10.1038/s41598-024-58066-y.

[54] B. Özdamar, Y. Sürmeli, and G. Şanlı-Mohamed, "Immobilization of Olive Leaf Extract with Chitosan Nanoparticles as an Adjunct to Enhance Cytotoxicity," *ACS Omega*, vol. 8, no. 32, pp. 28994–29002, 2023, doi: 10.1021/acsomega.3c01494.

[55] P. Sitarek, T. Kowalczyk, M. Owczarek, and L. Herczy, "Combination with Ginkgo biloba Extract in Preliminary In Vitro Studies," *Molecules*, vol. 28, no. 4950, pp. 1–15, 2023.

[56] T. İ. Horuz and K. B. Belibağlı, "Nanoencapsulation of carotenoids

extracted from tomato peels into zein fibers by electrospinning," *Journal of the Science of Food and Agriculture*, vol. 99, no. 2, pp. 759–766, 2019.

[57] N. E. A. El-Naggar, A. M. Shiha, H. Mahrous, and A. B. A. Mohammed, "A sustainable green-approach for biofabrication of chitosan nanoparticles, optimization, characterization, its antifungal activity against phytopathogenic Fusarium culmorum and antitumor activity," *Scientific Reports*, vol. 14, no. 1, pp. 1–23, 2024, doi: 10.1038/s41598-024-59702-3.

[58] T. T. George, A. B. Oyenihi, F. Rautenbach, and A. O. Obilana, "Characterization of moringa oleifera leaf powder extract encapsulated in maltodextrin and/or gum arabic coatings," *Foods*, vol. 10, no. 12, 2021, doi: 10.3390/foods10123044.

[59] S. M. Abdelaziz, F. M. M. Lemine, H. O. Tfeil, A. Filali-Maltouf, and A. O. M. S. Boukhary, "Phytochemicals, antioxidant activity and ethnobotanical uses of balanites aegyptiaca (L.) del. fruits from the arid zone of mauritania, Northwest Africa," *Plants*, vol. 9, no. 3, pp. 9–12, 2020, doi: 10.3390/plants9030401.

[60] N. E. A. El-Naggar, A. M. Shiha, H. Mahrous, and A. B. A. Mohammed, "Green synthesis of chitosan nanoparticles, optimization, characterization and antibacterial efficacy against multi drug resistant biofilm-forming Acinetobacter baumannii," *Scientific Reports*, vol. 12, no. 1, pp. 1–19, 2022, doi: 10.1038/s41598-022-24303-5.

[61] W. P. Dauda, "Antimicrobial Activity of Different Concentrations of Hexane Extract of Balanites aegyptiaca (l .) Delile (Desert Date) Kernel Oil International Journal of Microbiology and Applied Sciences Antimicrobial Activity of Different Concentrations of Hexane Extract of Balanites aegyptiaca (l .) Delile (Desert Date) Kernel Oil," no. September, 2023.

[62] P. Poznanski, A. Hameed, and W. Orczyk, "Chitosan and chitosan nanoparticles: parameters enhancing antifungal activity," *Molecules*, vol. 28, no. 7, p. 2996, 2023.

[63] A. Valian, H. Goudarzi, M. J. Nasiri, A. Roshanaei, and F. Sadeghi Mahounak, "Antibacterial and anti-biofilm effects of chitosan nanoparticles on Streptococcus mutans isolates," *Journal of Iranian Medical Council*, vol. 6, no. 2, pp. 292–298, 2023.

[64] L. M. Gradinaru, M. Barbalata-Mandru, A. A. Enache, C. M. Rimbu, G. I. Badea, and M. Aflori, "Chitosan Membranes Containing Plant Extracts: Preparation, Characterization and Antimicrobial Properties," *International Journal of Molecular Sciences*, vol. 24, no. 10, 2023, doi: 10.3390/ijms24108673.

[65] E. M. Costa, S. Silva, F. K. Tavaria, and M. Pintado, "Insights into the Biocompatibility and Biological Potential of a Chitosan Nanoencapsulated Textile Dye," *International Journal of Molecular Sciences*, vol. 23, no. 22, 2022, doi: 10.3390/ijms232214234.

[66] I. H. N. Bassolé and H. R. Juliani, "Essential oils in combination and their antimicrobial properties," *Molecules*, vol. 17, no. 4, pp. 3989–4006, 2012, doi: 10.3390/molecules17043989.

.